Journal of Safety Engineering 2016, 5(2): 27-35
DOI: 10.5923/j.safety.20160502.01

Energy Dissipation Measures on a Hockey Helmet across Impact Locations

Carlos Zerpa[1,*], Stephen Carlson[1], Siamak Elyasi[2], Eryk Przysucha[1], Thomas Hoshizaki[1]

[1]School of Kinesiology, Lakehead University, Thunder Bay, Canada
[2]Department of Chemical Engineering, Lakehead University, Thunder Bay, Canada

Abstract The objective of this study was to examine differences across hockey helmet impact locations on energy dissipation characteristics when mounted on a NOCSEA headform attached to a mechanical neck and drop carriage. Linear triaxial accelerometers mounted inside the headform were used to compute the energy dissipation across helmet impact locations. The amount of energy dissipated was calculated for five helmet impact locations including the front, front boss, side, rear boss, and rear. Inferential statistical analysis revealed significant differences in energy loading, $F(4,21)=19.727$, $p<0.005$, $\eta^2 = 0.78$ and energy unloading, $F(4,21)=56.793$, $\eta^2 = 0.91$ $p<0.005$ across impact locations. There were, however, no significant differences in the amount of energy dissipated across helmet impact locations, $F(4,21)= 2.033$, $p=0.126$. This outcome suggests that the hockey helmet mounted on a headform behaves differently on how it loads and unloads energy across impact locations, but appears to behave similarly across impact locations on the amount of energy dissipated due to an impact. These results may have implications on helmet testing and design because they shed light on the use of another measurement technique to assess the effectiveness of hockey helmets in minimizing risk of head injury due to an impact.

Keywords Concussion, Helmet Impact System, Energy Dissipation, Hockey Helmet

1. Introduction

Hockey is a fast and aggressive sport with high risk of injury [1]. The elevated risk of injury has lead to the development of new equipment technologies for injury prevention [2]. In the sport of hockey, helmets serve as the primary form of head protection [3]; however, injuries to the head and brain remain to be very common at the professional and amateur levels [4]. These types of injuries can be very severe in nature as they may lead to neurological dysfunction and in rare cases, death [5].

In the sport of hockey, helmets are designed to best protect the head against traumatic brain injuries (TBIs) such as skull fractures and subdural hematomas [3]. These severe injuries are caused by sudden accelerations and decelerations on the head and brain, resulting from mechanical impacts [6]. Designing a hockey helmet to prevent head injuries, however, involves many tradeoffs between performance, comfort, and appearance [7], making helmet design a difficult task to master.

Even since the mandatory wearing of helmets, head brain injuries continue to increase frequently in the sport of hockey. This increase in the frequency of head injuries may be due to mechanical constrains in the design and development of helmet materials and structures to provide protection to the athlete against head injuries. Furthermore, testing helmet protocols are not specific enough for the sport and have changed very little over the past 50 years [8, 9]. As stated in the literature, direct contact of the human head with an object during a fall or collision can cause serious brain injuries and skull fracture [10]. That is, if the deformation of the helmet is pushed past its threshold, mechanical failure can occur, which may lead to a skull fracture, epidural and subdural hematomas. These types of injuries cause brain bleeds, pressure gradients within the skull and great amount of intracranial damage [11]. While injuries like skull fracture in the sport of hockey have been largely eliminated with the implementation of helmets [12], these injuries still occur in rare cases [13].

According to the International Ice Hockey Federation (IIHF), there are 577 thousand hockey players registered and competing in different age groups and levels of competitiveness throughout Canada [14]. It was reported in 1999 that 3.78% of all sport related emergency room visits in Canada were due to head injuries that occurred while playing hockey. Most common of all these injuries were concussions; in fact, ice hockey has been identified as having the highest incidence of concussion and head injury per participant of all sports [15, 14]. When describing head injuries, they are generally categorized as focal or diffuse. Focal head injuries (e.g., skull fracture), relate to damage to a specific location of

* Corresponding author:
czerpa@lakeheadu.ca (Carlos Zerpa)
Published online at http://journal.sapub.org/safety

the brain. Diffuse head injuries (e.g. concussion) relate to damage to a more widespread portion of the brain.

There is little doubt that hockey helmets have been very effective in reducing the occurrence of head and brain injuries, especially those traumatic in nature [16]. The use of helmets in the sport of hockey has also led to the development of helmet testing protocols to assess the ability of the helmet to protect against concussions. Current methods for testing helmets involve a pass or fail criteria based on a single, large impact [5]. To conduct this testing, the helmet is usually mounted on a surrogate "headform", designed to respond closely to an actual human head. Accelerometers instrumented in the headform measure the peak linear acceleration felt by the headform during an impact [5]. A range of 275-300gs is used as a helmet failure criterion. This threshold was obtained from human cadaver research on skull fractures [17]. The unit "g" is used for any linear acceleration analysis and it is a multiple of the acceleration due to gravity ($g=9.81 m/s^2$). If the peak linear acceleration measured during the impact is less than the threshold acceleration measure, the helmet is deemed appropriately protective. While this measure of peak linear acceleration is based on the acceleration experienced by the brain through the centre of mass, this testing method may not be indicative of the rigor of the sport of hockey.

Current research in hockey helmet testing has also determined that rotational accelerations contribute to the occurrence of concussion and diffuse axonal injuries in the brain [18]. These rotational or angular accelerations are measured in a similar fashion as linear accelerations; but, are expressed in $rads/s^2$, or radians per second squared, which is a measure of changes in angular velocity over time. This type of acceleration is not generally included in initial testing protocols that evaluate the protective performance of a helmet.

Other researchers had examined the relationship between impact location and changes in peak linear accelerations as an avenue to better assess helmet performance. For example, Walsh, Rousseau, and Hoshizaki [21] demonstrated that impacts to different locations on a headform during testing revealed differences in peak linear accelerations. The researchers found that the side location produced the largest peak linear acceleration (132.8g) when compared to the front (121.3g) and rear locations (116.9g). Daniel, Rowson, and Duma [22], also observed the same relationship when analyzing real-life football impacts among youth participants.

While current measures of linear acceleration criteria have proven to be useful in the prediction of risk related to skull fracture and other severe head trauma [5], this measure remains a poor predictor of risk related to mild traumatic brain injuries (mTBI). A test focusing on energy dissipation across helmet impact locations should be examined to better understand injury mechanisms and the risk of injury during impact.

There is, however, little research work on the use of energy dissipation across helmet impact locations as an avenue to assess helmet performance and risk of injury. Energy dissipation analysis has been used in other studies to examine the protective ability of bicycle face protection and soccer headgear, but not of hockey helmet performance [23, 24]. Energy is dissipated by the helmet mainly through the attenuation layer, when energy is "absorbed" by the crushable foam [25].

Energy dissipation is defined as the conversion of mechanical energy into another form of energy, such as heat. An energy absorbing material would involve a loading and unloading curve [26], as shown in Figure 1. The area between the loading and unloading curves represents the energy dissipated by the foam during the impact. In an ideal situation, the foam would be loaded with the entirety of the incoming impact energy and all the energy would be dissipated out of the system during the unloading phase. This concept would suggest that all incoming energy generated during an impact would be absorbed and directed away from the head and brain.

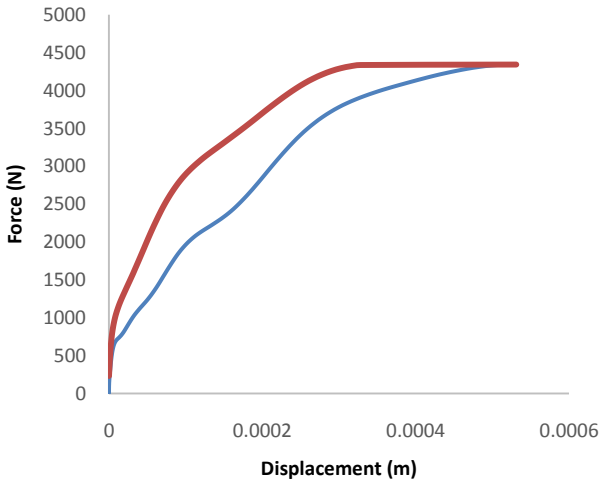

Figure 1. Example of energy loading and unloading curve during helmeted impact. The loading curve can be seen in red, while the unloading curve is shown as blue

Under this premise, an energy dissipation analysis may provide more information on helmet ability to protect the head against impacts. This type of analysis can shed light in defining a more robust measure for helmet designers to mitigate the occurrence of head and brain injuries. As stated by Barth, Freeman, Broshek, & Varney [27], a higher energy dissipation value can result in a lower rebound velocity, which in turn can result in a decreased chance of countercoup injury; a type of injury where the brain collides with the skull after impact.

2. Methods

2.1. Purpose

Based on the above rationale, the purpose of this study

was to examine the influence of impact location on the energy dissipation characteristics of a hockey helmet as compared to traditional measures of peak linear acceleration during simulated free falls.

2.2. Research Question

The following research question was used to guide the study:

What is the influence of helmet impact location on energy dissipation characteristics when mounted on a NOCSAE headform?

2.3. Instruments

Headform. A medium sized NOCSAE headform as depicted in Figure 2 was used for all impact trials. The headform was developed in order to simulate the dynamic response that a human head experiences during impact. This headform is considered to be more anatomically correct than the Hybrid III headform, which is another commonly used headform in the field of impact research. The NOCSAE headform is considered more anatomically correct due to the inclusion of appropriate facial features and bone structure. The NOCSAE headform is instrumented with an array of accelerometers to measure the acceleration felt at impact in the anterior-posterior, superior-inferior and left-right directions. This headform has been used in many published research studies to simulate the dynamic response of impact including both linear and rotational accelerations [5-7].

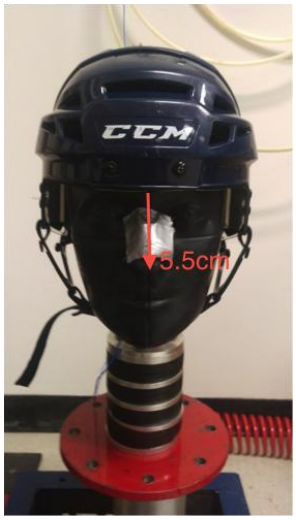

Figure 2. NOCSAE headform with properly fitted helmet. A distance of 5.5cm is measured between the brim of the helmet and the tip of the nose

Mechanical Neckform. The neckform, as depicted in Figure 3, was made of neoprene rubber with steel end plates in order to emulate the 50th percentile of a human neck. The neoprene rubber was designed to fit between circular steel disks. To prevent slippage between the steel and rubber disks, the constituent materials have a protruded cylindrical offset. The offset allows the steel and rubber disks to be pressed tightly together. A top plate and base bracket secure the components together.

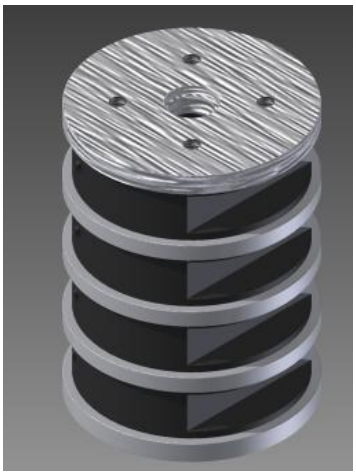

Figure 3. Mechanical neckform

The neoprene rubber, with steel end plates in the form of a neck was also designed to simulate neck inertial effects that occur during loading. Furthermore, the rubber disks were designed with two features of the human neck in mind. The first feature included a cutout of the cross-section of the disk. The second feature included a larger cutout in the back of the neck as depicted in Figure 3. These two processes were conducted to better mimic the features of a human neck and the loading response that a human neck would experience during an impact.

Helmets. Three CCM Vector V08 helmet (Figure 2) with VN attenuation liner were used during the testing to measure the energy dissipated during impact. Each helmet was best fitted on the headform prior to each drop by following helmet fitting instructions as defined by NOCSAE standards. Between each impact, the helmet was switched with another identical helmet to allow ample time for each helmet to rebound to its resting state. Figure 2 shows the CCM Vector V08 helmet mounted on the NOCSAE headform.

Drop system. An in-house dual rail drop system, as depicted in Figure 4, designed and constructed by students from the Lakehead Mechanical Engineering Department and staff from the faculty of the School of Kinesiology was used to conduct the helmet testing. The rig incorporates a drop carriage, to which the headform and neck can be mounted and secured on a minimal friction railing system, which behaves as free falling. The weight of the headform, neckform, and drop carriage is 30.6kg and remained as such throughout the entire procedures. A 110-volt AC winch with a wire connected to a magnetic plate was used to elevate the drop rig to the correct height prior to each impact. The winch raised or lowered the drop rig by using a switch mounted on an electronic controller. When the magnetic plate was energized, it remained in contact with the steel drop carriage. As soon as a release switch on the electronic controller was pressed, the magnets were deenergized and the drop carriage dropped freely on the impact anvil surface. The anvil impact surface was mounted on rubber matting and bolted into the floor to minimize noise and vibration caused during impact.

Figure 4. Drop system and impact anvil

Instron 1000 Mechanical Device. A modified Instron device was used to evaluate the mechanical properties of the helmet material due to compression during static loading for the front and side locations as depicted in Figure 5. The hardware of this device was upgraded by connecting the instrument to a data acquisition board from National Instrument and interfaced to the labview software to measures compressive or tensile forces and material deflection.

Figure 5. Instron 1000- test equipment for mechanical properties of materials

2.4. Procedures and Analyses

The helmet was tested statically using a technologically updated Instron 1000 device to assess the mechanical properties of the helmet at the front and side locations. A force was applied at either location using a 31.67 cm^2 cylinder with a diameter of 31.75 mm. The force and deflection data at each helmet location were recorded calibrated and computed via labview script and excel software.

The helmet was also tested dynamically. To conduct this test, the helmet was properly fitted on the headform prior to each drop by following helmet fitting instructions as defined by NOCSAE standards. To minimize wear and tear of the helmet material, the helmet was switched with an identical helmet after each impact to allow ample time for the impacted helmet to rebound to its resting state. Each identical helmet was impacted three times per location, similar to the research protocol used by Oeur, Hoshizaki, and Gilchrist [28]. The protocol used in the current study, however, included 5 locations as defined in NOCSAE drop test standards, but impacted at a velocity of 4.5m/s. The locations included in this testing protocol were the front, front boss, side, rear boss, and rear. For each impact location, the linear acceleration data (x, y, and z directions) captured by the accelerometers sensors mounted in the headform was fed into an analog to digital amplifier unit and processed via a commercial software package called POWERLAB.

Resultant linear acceleration was computed using the POWERLAB software calculation module based on Equation 1

$$\text{Resultant Acceleration} = \sqrt{x^2 + y^2 + z^2} \qquad (1)$$

where:

x = linear acceleration in the x-direction
y = linear acceleration in the y-direction
z = linear acceleration in the z-direction

A 1000 Hz low pass filter was implemented to minimize noise levels. The data were collected at a sampling rate of 20,000 Hz for each acceleration input channel composed of 12 bit data. Each helmet location was tested in sequential order, ensuring that all impacts to each helmet were completed before moving to the next location. The order of impacts was front, front boss, side, rear boss, and rear as defined by NOCSAE standards. A total of 45 impacts were applied among the three helmets. The linear acceleration data captured by the headform in combination with the mass of the drop carriage, headform, neck and helmet were used to compute the loading and unloading energy during the impact. To obtain these computations of energy, the impact force was calculated using Equation 2.

$$F = m.a \qquad (2)$$

where:

F = force due to the impact
m = mass of drop carriage, headform, neck and helmet
a = resultant acceleration measured by accelerometres

Next, the velocity during the impact was calculated using Equation 3.

$$V_f(t) = V_i + \frac{1}{m}\int_0^t F \cdot dt \qquad (3)$$

where:

$V_f(t)$ = final velocity during the impact
V_i = initial velocity during the impact

M = mass of drop carriage, headform, neck and helmet
F = due to the impact
T = time duration of impact
dt = sampling time

Follow to the calculations of velocity during the impact, the change in displacement for the duration of the impact was calculated using Equation 4.

$$s(t) = s(t_0) + \int_{t_0}^{t} V_f(t).dt \quad (4)$$

where:
s(t) = change in position
$s(t_0)$ = initial position
t_0 = time at beginning of interval
t = time at end of interval
V_f = velocity
dt = sampling time

Finally, the loading and unloading energy during the impact was calculated based on Equations 5 and 6.

$$E_{Loading} = \int_{0}^{s} F_1 \cdot ds \quad (5)$$

where:
$E_{Loading}$ = energy produced due to the deformation of material shape at impact
F_1 = force of action to deform the material shape at impact
ds = compression interval
S = total displacement of material due to deformation

$$E_{Unloading} = \int_{0}^{s} F_2 \cdot ds \quad (6)$$

where:
$E_{Unloading}$ = energy produce to restore the material shape at impact
F_2 = force of reaction to restore material shape due to the impact
ds = decompression interval
S = total displacement of material due to restoring its shape.

The energy dissipated during the impact was calculated by subtracting the unloading energy from the loading energy. The percent of energy dissipation was calculated by the dividing the energy dissipated over the loading energy for each impact location. One-way ANOVAs were conducted to determine if differences existed in energy loading, unloading and dissipation across impact locations.

3. Results

Static measures of helmet stiffness were conducted for the front and side locations as depicted in Figure 6 and 7. The outcome obtained from the ratio calculation of the 2 regression curve slopes (ratio=*1.66/0.67*) indicate that the front location requires 2.48 times more force to acquire the same deflection as the side location. That is, the helmet has stiffer material properties at the front location than the side location.

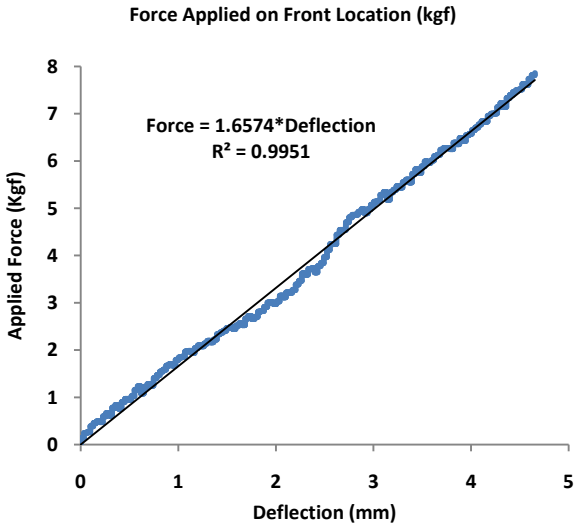

Figure 6. Force-Deflection Curve for Front Location of Helmet. The figure shows the static loading characteristics of the helmet material at the front location to determine stiffness properties

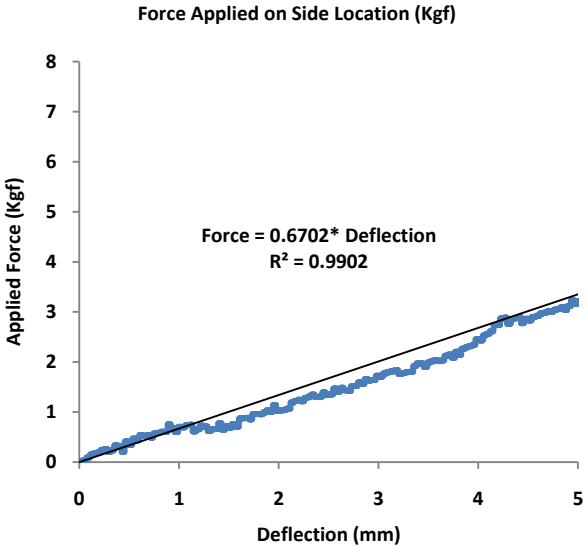

Figure 7. Force-Deflection Curve for Side Location of Helmet. The figure shows the static loading characteristics of the helmet material at the Side location to determine stiffness properties

Dynamic measures of peak linear acceleration and energy were collected across all helmet impact locations. These measures are depicted in Tables 1 and 2. The results as depicted in Table 1 indicate that the mean peak linear acceleration is the highest at the front boss (FB) location (M=136.42g, SD= 17.36g) and lowest at the rear location (M=125.10g, 4.31g).

Table 1. Peak Linear Accelerations across Impact Locations

Location	Mean (g)	SD (g)
Front	112.23	6.14
Front Boss	136.41	17.36
Side	108.38	6.82
Rear Boss	125.37	3.74
Rear	125.10	4.31

The results as shown in Table 2 also indicate that the mean energy loading (46.259 J) and unloading (37.010 J) due to each impact are higher at the front boss location (46.259 J) when compared to the other impact locations. The front boss, however, only dissipates 10.437% of the energy loaded into the system including the head, neck and helmet. The energy loading and unloading for a front boss impact location can be seen in Figure 8.

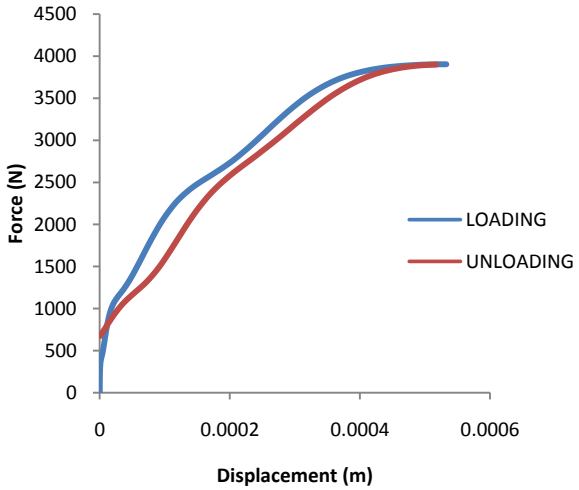

Figure 8. Force-Displacement Curve for Front Boss Impact. The figure shows the energy loading and unloading characteristics typical of the front boss impact location

The results for the front location as depicted in Table 2, indicate that the mean energy loading (42.744 J) and unloading (37.010 J) are lower than the front boss location. The energy dissipation at the front location represents 13.414% of the total energy loaded into the system due to an impact, which seems to be 2.97% more efficient in energy dissipation when compared to the front boss location. A force-displacement curve for a front impact location can be seen in Figure 9.

The results for the side location as depicted in Table 2, indicate that the mean energy loading (45.917 J) and unloading (35.810 J) are lower than the front boss location, but higher in energy loading than the front location. The energy dissipation at this location represents 22.011% of the total energy loaded into the system due to an impact, which seems to be the most efficient location on the helmet in energy dissipation according to these data. A force-displacement plot for a side impact can be seen in Figure 10.

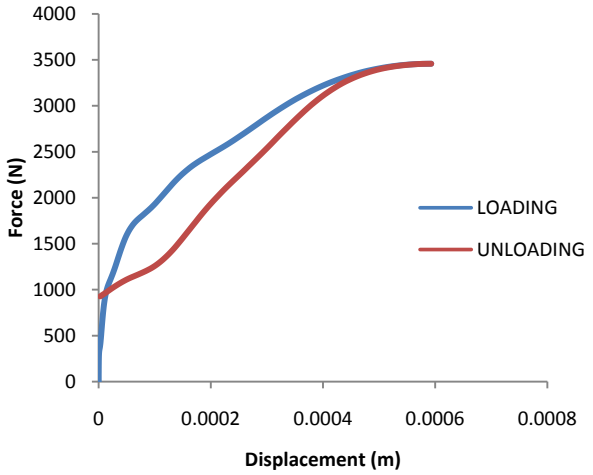

Figure 9. Force-Displacement Curve for Front Impact Location. The figure shows the energy during the loadding and unloading phases of the impact

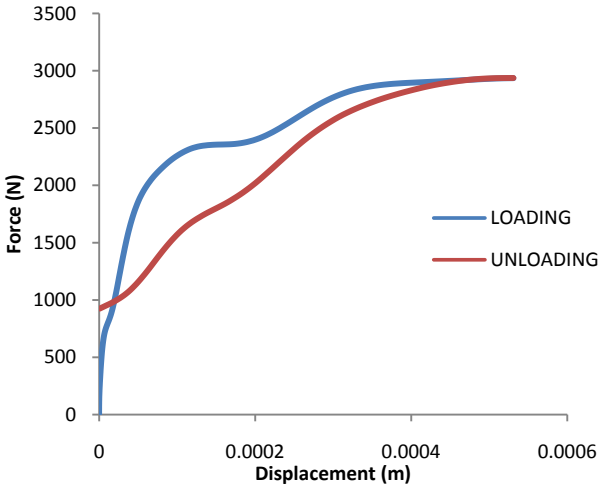

Figure 10. Force-Displacement Curve for Side Impact Location. The figure shows the energy loading and unloading characteristics of an impact to the side impact location

The results for the rear boss location as depicted in Table 2, indicate that the mean energy loading (21.697 J) and unloading (17.998 J) are the lowest among all impact locations. The energy dissipation at this location represents 17.048% of the total energy loaded into the system due to an impact, which seems to be the second most efficient location on the helmet in energy dissipation according to these data.

A force-displacement curve for a rear boss impact location can be seen in Figure 11.

The results for the rear location as depicted in Table 2, indicate that the mean energy loading (32.952 J) and unloading (27.887 J) are the second lowest among all impact locations. The energy dissipation at this location represents 15.370% of the total energy loaded into the system due to an impact, which seems to be less efficient in energy dissipation when compared to the rear boss location according to these data. A force-displacement curve for a rear impact can be seen in Figure 12.

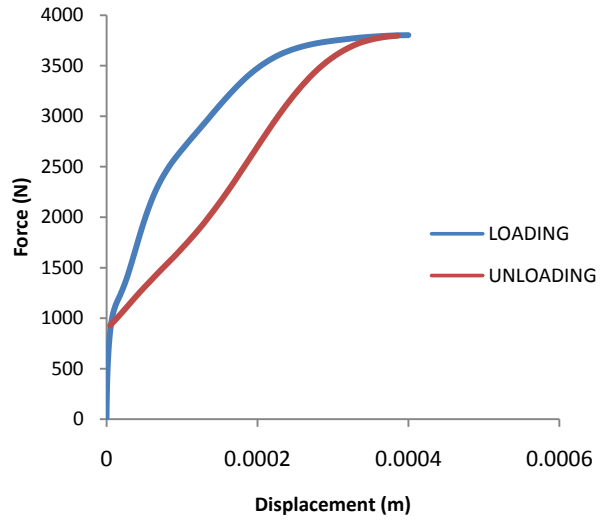

Figure 11. Force-Displacement Curve for Rear Boss Impact Location. The figure shows the loading and unloading energy curves during impact

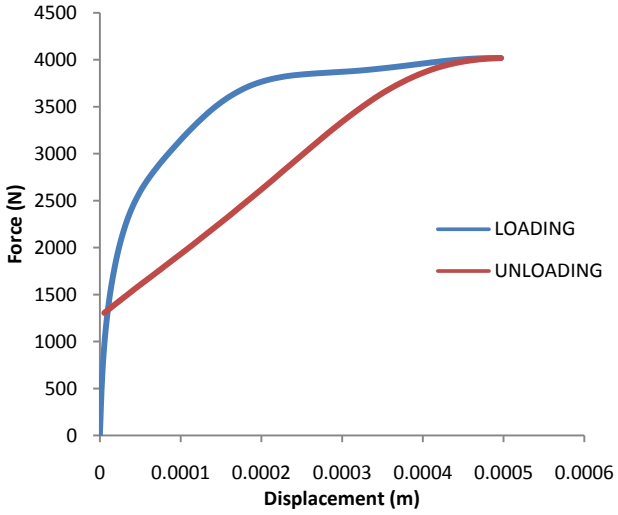

Figure 12. Force-Displacement Curve for Rear Impact Location. The figure shows the energy loading and unloading characteristics of an impact to the rear of the helmet

Table 2. Energy Dissipation Characteristics of Impact Locations

Location	Loading (J)	Unloading (J)	Dissipated (J)	% Dissipated
Front	42.744	37.010	5.734	13.414
Front Boss	46.259	41.414	4.845	10.473
Side	45.917	35.810	10.107	22.011
Rear Boss	21.697	17.998	3.699	17.048
Rear	32.952	27.887	5.064	15.370

One-way ANOVAs were conducted to determine if there were significant differences in energy loading, unloading, and dissipation across the impact locations tested. The results indicate significant differences in energy loading, $F(4,21)=19.727$, $p<0.005$, $\eta^2 = 0.91$ and energy unloading, $F(4,21)=56.793$, $p<0.005$, $\eta^2 = 0.78$ both with a large effect size η^2 (eta square) across impact locations. There were, however, no significant differences in energy dissipation, $F(4,21)=2.033$, $p=0.126$ and percent energy dissipation, $F(4,21)=1.534$, $p=0.229$ across impact locations.

4. Discussion

When analyzing helmet performance using traditional kinematic measures of peak linear acceleration, there appear to be differences in helmet protective ability across impact locations. In the current study for example, the front boss location resulted in the largest amount of peak linear acceleration and the side location resulted in the lowest amount of peak linear acceleration when they were impacted at the speed of 4.5 m/s. Differences across locations on a headform impacted without a helmet at the speed of 5.5 m/s had also been found in previous research [21, 22], but with the side location generating the highest peak linear acceleration. Discrepancies on which location generates the highest or lowest peak linear acceleration when comparing previous research to the current findings may be related to helmet properties and impact velocity. These discrepancies, however, suggest that the helmet properties change the behaviour of the headform and neck, and consequently, minimize the risk of injury across impact locations.

The effect of helmet geometry to accommodate comfort and appearance also appears to influence the behaviour of the helmet across impact locations [7]. As the results of the current study indicate, identical impacts across five helmet locations revealed a higher peak linear acceleration for the front boss location and consequently a greater risk of injury at this location. The side helmet location, however, appears to be the most protective against head trauma as it generated the least amount of peak linear acceleration. This outcome is also supported by the static testing conducted on the helmet, which revealed that the helmet is more flexible (more deformation due to a specific force) on the side locations when comparing it to the front location.

The energy analysis conducted in this study to determine the influence of helmet properties on the amount of energy dissipated across impact locations also supports the findings obtained with traditional measures of peak linear acceleration. As the results indicate, less energy was dissipated at the front boss location, which related to a higher peak linear acceleration when compared to other impact locations as shown in Table 1 and 2. Similarly, more energy was dissipated at the side location, which related to a lower peak linear acceleration when compared to other impact locations. Although no significant differences were found on energy dissipation across impact locations when conducting the ANOVA, the outcome of this study based on descriptive statistical analysis supports the existing literature. That is, a higher energy dissipation value can result in a lower rebound velocity, which minimizes the chance of brain injury [27].

One advantage of using an energy analysis to examine helmet performance instead of just traditional measures of

peak linear acceleration is that, an energy analysis offers an avenue to examine the dynamic response of the helmet material properties in dissipating energy across impact locations. That is, this approach accounts for the force generated during an impact and the deflection of the helmet material to withstand this force at each location, which is very useful information to understand the injury mechanism [6] and the behaviour of the helmet material, as an avenue to possibly improve the protective ability of the helmet.

From the structural design perspective, an energy dissipation analysis can provide more information on the behaviour properties of the helmet material locations during impact testing. This information can help helmet manufactures improve weaker helmet areas to better dissipate energy, decrease the rebound velocity and minimize the risk of brain tissue damage during head impacts. As stated by Barth [27], lower rebound velocity during helmet impacts minimizes the risk and occurrence of secondary impact mechanisms, which are also considered to be responsible for post-concussion syndrome and chronic traumatic encephalopathy (CTE). CTE is a rare progressive neurological disorder that can result in cognitive, mood, behavioral, and neurological symptoms negatively affecting the lives of athletes [29].

There are, however, limitations in this study when conducting the energy analysis. One of the main limitations is that we did not compute the energy dissipated by the helmet itself across impact locations, but rather the energy dissipated by the helmet, headform and neck across impact locations. To compute the energy dissipated by the helmet itself, similar impacts need to be conducted on the headform with and without a helmet. Differences between energy computations obtained with and without a helmet will indicate the amount of energy absorbed by just the helmet. The issue, however, is that conducting impacts on a bare headform will more likely cause damage to the mechanical structure of the headform designed to simulate the anatomical structure of a human head.

Another limitation of the current technique is that the calculations of energy are computational intensive and time consuming, which require the creation of computer software scripts in excel, matlab or other computer software languages. As opposed to traditional measures of peak linear acceleration used to assess helmet performance, in which the measure of linear acceleration is obtained directly from the accelerometer sensors after implementing calibration and noise filtering. Furthermore, the current model only uses one type of helmet brand. Other helmet brands may behave differently across helmet impact locations on energy dissipation. This study, however, sheds light on the use of energy dissipation as a measurement technique, which can be applied to other helmet brands to better understand a helmet protective ability against head injuries.

Finally, we did not conduct an energy analysis across impact locations for different impact velocities to examine the effect of speed and helmet impact location on energy dissipation. It is an idea that we want to implement for future research. It is also important to mention that the current study did not include measures of rotational acceleration, which are considered to be a contributor to the occurrence of concussions and the diffuse of axonal injuries in the brain. The reason for not including measures of rotational acceleration in the current study was due to hardware limitations. But also, because, we were more interested in comparing energy dissipation measures to traditional measures of peak linear acceleration, which are used as standard criteria to assess hockey helmet pass or fail performance during impact testing.

5. Conclusions

The purpose of this study was to determine the influence of helmet impact location on the amount of energy dissipated during simulated impacts when compared to traditional measures of peak linear acceleration. The results indicate differences across impact locations on energy and acceleration measures.

From the theoretical and practical perspective, the outcome of this study supports and builds on existing literature [16, 17, 22] and provides another avenue for researchers and helmet manufacturers to assess helmet performance in addition to traditional measures of peak linear acceleration. As previously stated in the literature [3], the idea is to design a helmet to best protect the head against head trauma induced by acceleration and decelerations to head from an impact.

The measures of energy obtained in the current study provide a clear trace of the helmet material properties on energy loading, unloading and dissipation to better understand injury mechanisms and deformation of helmet material due to a head impact. In summary, this approach offers an avenue to better understand mechanical failures of helmets when pushed beyond its threshold. Information that is useful in helmet designs to minimize risk of head injuries and possibly the risk of mild traumatic brain injuries.

REFERENCES

[1] Flik, K., Lyman, S., & Marx, R. (2005). American collegiate men's ice hockey: an analysis of injuries. *American Journal of Sports Medicine, 33*(2), 183-187.

[2] Wennberg, R., & Tator, C. (2003). Nation Hockey League reported concussions, 1986-87 to 2001-02. *Canadian Journal of Neurological Science, 30*(3), 206-209.

[3] Kis, M., Saunders, F., Kis, M., Irrcher, I., Tator, C., Bishop, P., & Hove, M. (2013). A method of evaluating helmet rotational acceleration protection using the Kingston Impact Simulator (KIS Unit). *Clinical Journal of Sports Medicine, 23*(6), 470-477.

[4] Benson, B., Mieeuwisse, W., Rizos, J., Kang, J., & Burke, C. (2011). A prospective study of concussions among National

Hockey League players during regular season games: the NHL-NHLPA Concussion Program. *Canadian Medical Association Journal, 183*(8), 905-911.

[5] Post, A., Oeur, A., Hoshizaki, B., & Gilchrist, M. (2011). Examination of the relationship between peak linear and rotational accelerations to brian deformation metrics in hockey helmet impacts. *Computer Methods in Biomechanics and Biomedical Engineering, 16* (5), 511-519.

[6] Namjoshi, D., Good, C., Cheng, W., Panenka, W., Richards, D., Cripton, P., & Wellington, C. (2013). Towards medical management of traumatic brain injury: a review of models and mechanisms from a biomechanical perspective. *Disease Models and Mechanisms, 6*(6), 1325-1338.

[7] Graham, R., Rivara, P., Ford, M., & Spicer, C., (2014). *Sports-Related Concussion in Youth.* Washington, DC: The National Academies Press.

[8] Rowson, B., Rowson, S., & Duma, S. (2015). Hockey STAR: A methodology for assessing the biochemical performance of hockey helmets. *Annals of Biomedical Engineering, 43*(10), 2429-2443.

[9] Halstead, D., Alexander, C., Cook, E., & Drew, R. (1998). "Hockey Headgear and the Adequacy of Current Design Standards". Safety in Ice Hockey, ASTM STP 1341, Ashare, A., B., Ed., ASTM International, West Conshohocken, PA, 2000, pp. 93-100.

[10] Yoganandan, N., & Pintar, F. (2004). Biomechanics of temporo-parietal skull fracture. *Clinical Biomechanics, 19*(3), 225-239.

[11] Gurdjian, E., Webster, J., & Lissner, H. (1955). Observations on the mechanism of brain concussion, contusion, and laceration. *Journal of Surgery, Gynecology, and Obstetrics, 101*(6), 680-690.

[12] Post, A., Oeur, A., Hoshizaki, B., & Gilchrist, M. (2011). Examination of the relationship between peak linear and rotational accelerations to brian deformation metrics in hockey helmet impacts. *Computer Methods in Biomechanics and Biomedical Engineering, 16*(5), 511-519.

[13] Honey, C. (1998). Brain injuries in ice hockey. *Clinical Journal of Sports Medicine, 8*(1), 43-46.

[14] Kendall, M., Post, A, Rousseau, P., Gilchrist, M., & Hozhiaki, B., (Eds). (2012). A comparison of dynamic impact response and brain deformation metrics within the cerebrum of head impact reconstructions representing three mechanisms of head injury in ice hockey. *Proceedings from IRCOBI 2012*: *International Research Council on the Biomechanics of Injury*. Dublin, Ireland: University of Dublin.

[15] Kelly, K., Lissel, H., Rowe, B., Vinventen, J., & Voaklander, D. (2001). Sport and recreation-related head injuries treated in the emergency department. *Clinical Journal of Sports Medicine, 11*(2), 77-81.

[16] Hoshizaki, B., & Chartrand, D. (Eds.). (1995). *Proceedings from ISBS-1995: 13th International Symposium on Biomechanics in Sport*. Thunder Bay, ON: Bauer.

[17] Gurdjian, E., Roberts, V., & Thomas, L. (1966). Tolerance curves of acceleration and intracranial pressure and protective index in experimental head injury. *Journal of Trauma, 6*, 600-604.

[18] King, A., Yang, K., Zhang, L., & Hadry, W. (Eds). (2003). Is head injury caused by linear or rotational acceleration? Proceedings from IRCOBI 2003: *International Research Council on the Biomechanics of Injury*. Lisbon, Portugal.

[19] Zhang, L., Yang, K., & King, A. (2011). Comparison of brain responses between frontal and lateral impacts by finite element modeling. *Journal of Neurotrauma*, *18*(1), 21-30

[20] Gennarelli, T., Thibault, L., Adams, J., Graham, D., Thompson, C., & Marcincin, R. (1982). Diffuse axonal injury and traumatic coma in the primate. *Annals Of Neurology, 12*(6), 564-574.

[21] Walsh, E., Rousseau, P., & Hoshizaki, T. (2011). The influence of impact location and angle on the dynamic impact response of a Hybrid III headform. *Sports Eng, 13*(3), 135-143.

[22] Rowson S, Duma S. The temperature inside football helmets during head impact: a five-year study of collegiate football games. *Proceedings of the Institution of Mechanical Engineers, Part P: Journal of Sports Engineering and Technology*. 2013, *227*(1), 12-19.

[23] Marsh, P., McPherson, M., & Zerpa, C. (Eds.). (2004). *Proceedings from ISBS-2004: 22nd International Symposium on Biomechanics in Sport*. Ottawa, ON.

[24] Monthatipkul, S., Iovenitti, P., & Sbarski, I. (2012). Design of facial protection gear for cyclists. *Journal of Transportation Technologies, 2*, 204-212.

[25] Cui, L., Kiernan, S., & Gilchrist, M. (2009). Designing the energy absorption capacity of functionally graded foam materials. *Materials Science and Engineering, 30*, 3405-3413.

[26] McLean, A., FIldes, B., Kloeden, C., Digges, K., Anderson, R., Moore, V., Simpson, D., "Prevention of Head Injuries to Car Occupants: An Investigation of Interior Padding Options," University of Adelaide, 1997.

[27] Barth, J., Freeman, J., Broshek, D., & Varney, R. (2015). Acceleration-deceleration sport-related concussion: The gravity of it all. *Journal Of Athletic Training, 36*(3), 253–256.

[28] Oeur, A., Hoshizaki, T., Gilchrist, M. The influence of impact angle on the dynamic response of a Hybrid III headform and brain tissue deformation. 2012, ASTM conference 2012, published by ASTM International.

[29] Concannon, L., Kaufman, M., & Herring, S. (2014). Counseling athletes on the risk of chronic traumatic encephalopathy. *Sports Health, 6*(5), 396-401.